

論文 A Unified Solidification Model of Hardening Concrete Composite at an Early Age

Rasha MABROUK^{*1}, Tetsuya ISHIDA^{*2}, and Koichi MAEKAWA^{*3}

ABSTRACT: A solidification model based on the micro-physical information for the prediction of both creep and shrinkage of hardening young concrete was previously introduced. Further modifications of some of the model parameters are proposed. Two-point loading experiments were conducted on concrete beams in order to verify the model proposed in the structure level. The data obtained are shown and compared with the analytical results.

KEYWORDS: young concrete, shrinkage, creep, multiphase material, microphysics, solidification, cement paste, stiffness

1. INTRODUCTION

The early stage of concrete life is known to have a significant control on the overall performance of concrete structures. In fact, it can be said that the future of a reinforced concrete structure may be partly decided based on the information obtained from this period. During this stage, concrete may be subjected to severe internal actions due to thermal and hygric gradients within the concrete itself and at the same time it may be affected by the external conditions of environment and loading. All these actions may lead to different deformations within the concrete that is just building its resistance and stiffness. All this makes it of great importance to be able to correctly predict the early age behavior of these structures. This research tries to deal with these behaviors using only one microphysical model in a unified manner [1,2]. As the model proposed showed good future prospect [1], therefore, further enhancement of some of the model parameters is attempted based on experimental data conducted on pure cement paste specimens. An attempt to utilize the solidification model in the prediction of the overall structure behavior is done by conducting experiments on concrete beams. The output from the analysis conducted using the proposed model and the results of experiments are compared together.

2. THE ANALYTICAL MODEL

In this research, concrete is idealized as a two-phase solid dispersion system, namely cement paste and aggregate. The total deformation of concrete is divided into two components, that is to say, volumetric component and deviatoric one. Concerning the volumetric component, five simultaneous equations are used to represent both the system of aggregate and cement paste [1,2] as shown in eq. (2) to eq. (6).

Virtual work principle, basically, Green's formula for the conversion of volumetric divergence

^{*1} Department of Civil Engineering, University of Tokyo, Ph. D., Member of JCI

^{*2} Department of Civil Engineering, University of Tokyo, Dr. E., Member of JCI

^{*3} Department of Civil Engineering, University of Tokyo, Prof., Dr. E., Member of JCI

to the surface outer stream integral, was utilized for theoretically deriving the mean stress and strain on the cement paste and aggregate. As for aggregate, it is assumed as a linear elastic material suspended in the cement paste. The solidification concept [3] is used to represent the behavior of cement paste. Fig. 1 shows a schematic representation of the overall system at an arbitrary stage.

$$\bar{\epsilon}_o = \frac{1}{3}(\epsilon_{xx} + \epsilon_{yy} + \epsilon_{zz}) \quad (1)$$

$$\bar{\epsilon}_o = \rho_{ag} \bar{\epsilon}_{ag} + \rho_{cp} \bar{\epsilon}_{cp} \quad (2)$$

$$\bar{\epsilon}_{cp} = f(\bar{\sigma}_{cp}) \quad (3)$$

$$\bar{\epsilon}_{ag} = \frac{1}{3K_{ag}} \bar{\sigma}_{ag} \quad (4)$$

$$\left(\frac{\bar{\sigma}_{ag} - \bar{\sigma}_{cp}}{G_{cp}} \right) + (\bar{\epsilon}_{ag} - \bar{\epsilon}_{cp}) = 0 \quad (5)$$

$$\bar{\sigma}_o = \rho_{ag} \bar{\sigma}_{ag} + \rho_{cp} \bar{\sigma}_{cp} \quad (6)$$

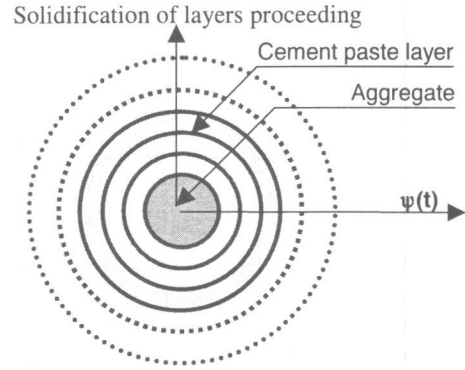


Fig. 1 Schematic representation of aggregate and cement paste

where, ϵ_{xx} , ϵ_{yy} and ϵ_{zz} are the strains in the direction of the x, y and z axes, $\bar{\sigma}_o$, $\bar{\sigma}_{ag}$ and $\bar{\sigma}_{cp}$

are the mean volumetric stresses on concrete, aggregate and cement paste, respectively, and $\bar{\epsilon}_o$, $\bar{\epsilon}_{ag}$ and $\bar{\epsilon}_{cp}$ are the mean volumetric strains, ρ_{ag} and ρ_{cp} are the volume fractions of aggregate and cement paste, respectively. K_{ag} is the volumetric stiffness of the aggregate and G_{cp} is the shear stiffness of cement paste. Function f will be discussed in detailed in section 2.1.

As for the deviatoric component, a similar procedure is assumed. For simplicity and assuming free rotation of the suspended particles, the shear component of suspended aggregate can be neglected. Therefore the shear strains and stresses of concrete are equal to those of the cement paste phase. In this case, the system is finally reduced to one equation, which is the constitutive relation for cement paste. Here, tensorial formulation is used as shown in eq. (7) and eq. (8). Finally, the total stress tensor for concrete, σ_{ij} , can be calculated by using eq. (9).

$$e_{ij} = \epsilon_{ij} - \bar{\epsilon}_o \delta_{ij} \quad (7)$$

$$S_{ij} = f(e_{ij}) \quad (8)$$

$$\sigma_{ij} = S_{ij} + \sigma_o \delta_{ij} \quad (9)$$

where, ϵ_{ij} is the total strain tensor for concrete and S_{ij} and e_{ij} are the deviatoric stress and strain tensors for cement paste, respectively. δ_{ij} is the Kronecker's delta function.

2.1 MODELING OF CEMENT PASTE

Fig. 2 shows the solidifying model for the assumed cement paste layers. In this research, it is assumed that new layers of cement paste solidify one by one according to the hydration development. When, the total volume of cement paste is V_{cp} and the effective volume solidified at time t is $V(t)$, the ratio of hydration controlling the solidification of layers is $\psi(t) = V(t) / V_{cp}$. The layers of cement paste are assumed to join in parallel

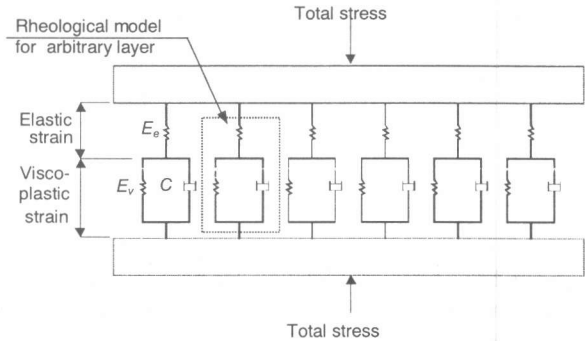


Fig. 2 Solidifying model for cement paste layers

where each layer is represented using two simple springs and a dashpot system. Thus, the total stress in cement paste at a certain time is the summation of the stress in the individual layers found at that time as shown in equations (8) and (9). The constitutive relation for each layer is shown in Fig. (2) and can be obtained using the rate type creep law as shown in equations (10) and (11).

$$\text{Volumetric part:} \quad \bar{\sigma}_{cp}(t) = \int_{t'=0}^t S_{cp}(t', t) d\psi(t') \quad (8)$$

$$\text{Deviatoric part:} \quad S_{ij}(t) = \int_{t'=0}^t S_{ij}(t', t) d\psi(t') \quad (9)$$

$$\text{Volumetric part:} \quad \left(1 + \frac{E_v}{E_e}\right) S_{cp}(t) + \frac{C}{E_e} \frac{dS_{cp}(t)}{dt} = E_v \bar{\epsilon}'_{cp}(t) + C \frac{d\bar{\epsilon}'_{cp}(t)}{dt} \quad (10)$$

$$\text{Deviatoric part:} \quad \left(1 + \frac{G_v}{G_e}\right) S_{ij}(t) + \frac{V}{G_e} \frac{dS_{ij}(t)}{dt} = G_v \cdot e'_{ij}(t) + V \frac{de'_{ij}(t)}{dt} \quad (11)$$

where, S_{cp} and S_{ij} are the average volumetric stress and the deviatoric stress tensor for cement paste, respectively. $\bar{\epsilon}'_{cp}(t)$ is the volumetric strain of cement paste in a general layer, E_e and E_v are the stiffness of the elastic and the plastic springs, respectively. $e'_{ij}(t)$ is the deviatoric strain tensor in a general layer, G_e and G_v are the shear stiffnesses and C and V are the constants of the dashpot fluid for volumetric and deviatoric components, respectively.

The elastic stiffness of each layer is calculated such that the summation of stiffness over all layers at a certain time is equal to that of cement paste at this time. The plastic stiffness of each layer, E_v , is taken as 1/3 of the elastic stiffness of that layer. It can be seen from the above that there are two important parameters controlling the behavior of each layer. That is, the stiffness of cement paste and the dash pot parameter C .

(1) The stiffness of the cement paste (E_{cp})

In order to properly model cement paste, necessary and sufficient parameters are needed. The most important of these are the strength and the stiffness of the paste. At first, the strength and the stiffness of cement paste were approximately assumed as a function of the concrete strength and stiffness. However, the stiffness and strength development could not be correctly predicted at the early age using this approximation and consequently, the concrete deformations were not properly estimated. Therefore, a more appropriate method should be used. In this research, simple experiments were conducted that were aimed at determining these two properties for different cement types.

Two cement types were used namely; ordinary portland cement and moderate heat cement. For each type of cement, three specimens were tested at the age of 1,2,3,7,14,21 and 28 days. For each case, two water to cement ratios was tested; that is 0.3 and 0.4. Cylinder specimens of size 5x10 cm were used. The specimens were cast under ordinary room temperature. After casting, the specimens were sealed then stored in the controlled environment room under temp of 20 °C and relative humidity of 60 % until the day of testing. The weight of sample specimens was monitored. On the day of the test, the specimens were removed from the environment room and the sealing was removed. The specimens were loaded under compression until failure. The strain was recorded at constant load increments. The peak load was also determined. The average of each three specimens was computed.

The output from the tests was the compressive strength and the stiffness of the cement paste. In the analysis, these strength and stiffness of cement paste are represented using the number of the assumed solidified layers. Using a thermo-dynamical program DuCOM [4], the effective porosity of paste was numerically computed at each time of testing. Compressive strength was correlated against this effective porosity as shown in Fig. (3). Similarly, the stiffness was correlated against compressive strength as shown in Fig. (4).

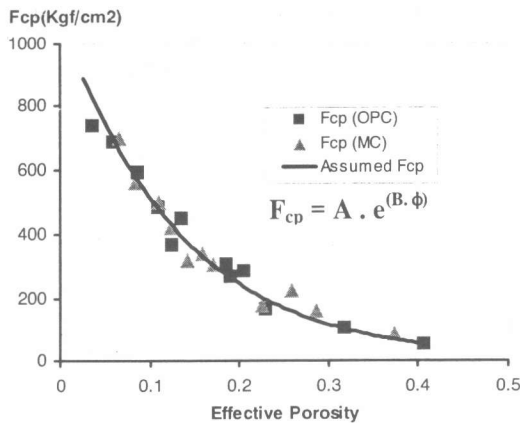


Fig. 3 Compressive strength of cement paste vs. effective porosity (ϕ).

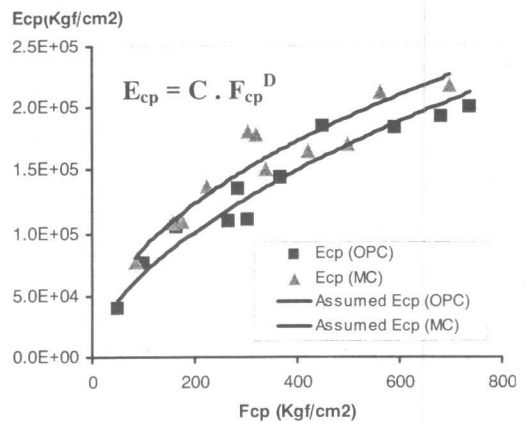


Fig. 4 Stiffness of cement paste vs. compressive strength.

(2) The dash pot parameter (C & V)

The dashpot constant is assumed to be related to the water motion through the pores associated with thermo-hygro-physical requirements. In this analysis, it is assumed as a function in the saturation degree, the viscosity of paste water and the porosity as shown in eq. (12). Initially a simplified linear relation was used between the dashpot constant and the saturation but now, it is replaced by the curve shown in Fig. (5). When the saturation degree is very low, almost no motion of water occurs and thus the dashpot parameter is almost zero. As the saturation degree increases, the dashpot parameter increases until a certain value where it is kept constant.

$$C = V = a \cdot f(S) \cdot \eta^b \cdot \phi^c \quad (12)$$

where, a is a constant and can be assumed as 2.0×10^6 , ϕ is the total porosity of the paste related to this arbitrary layer, S is the total saturation of the paste for the layer, η is the viscosity of the water in the micropores [5] and b & c are constants taken as 1 and -1 , respectively. Function, f , can be defined as shown in Fig. (5).

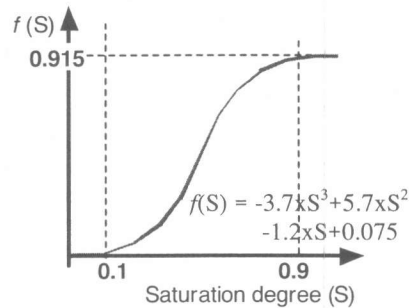


Fig. 5 Variation of dash pot constant against saturation degree

2.2 COUPLING OF SKELETON STRESSES AND PORE WATER PRESSURE

Capillary tension has been introduced by many of the past researchers as the source of shrinkage behavior [6]. Under this assumption the volume change and the deformation of cement paste will occur due to the surface tension force of capillary water across curved meniscus. In this study, the combined effect of external loads and pore water pressure created by the micro-scale surface tension is treated as the driving force for the deformation of concrete. Accordingly, the total average volumetric stress on concrete $\bar{\sigma}_{ot}$ is calculated by using eq. (13).

$$\bar{\sigma}_{ot} = \bar{\sigma}_o + 0.8 \times S \times P \quad (\text{pore water radius, surface tension of liquid water}) \quad (13)$$

where, P denotes pore water pressure and S denotes the saturation degree, both of which are computed by the thermo-hygro-physical approach [5].

3. EXPERIMENTAL WORK

For further verification of the model, a series of experiments on concrete beams is conducted. The details of the beams studied are shown in Table (1) and Fig. (7). The specimens were cast under ordinary room temperature. After casting, the specimens were sealed. On the day of the experiment, the specimens were exposed to the environment and the load was applied.

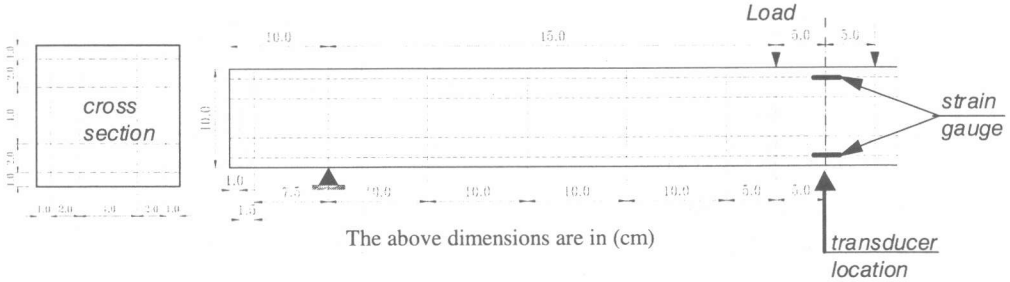


Fig. 7 The FEM mesh used in the analysis and the location of the measuring instruments

Table (1) General information of the test specimens

Beam No.	W/C	ρ^*_{agg}	Cement Type**	Environmental conditions	Load- ing	f_c^{***} (Pa)	Load (N)
B1	40%	68%	MC	RH of 67% at age = 3 days	3 days	-	1100.0
B2	40%	68%	OPC	RH of 67% at age = 3 days	3 days	-	1150.0
B3	40%	50%	MC	RH of 61% at age = 4 days	4 days	0.280	1060.5
B4	30%	68%	MC	RH of 67% at age = 3 days	3 days	0.400	1060.5

(* The ratio of total aggregate, sand and gravel, by volume), (** OPC = Ordinary Portland Cement & MC = Moderate Heat Cement), (***) Compressive strength at the age of loading)

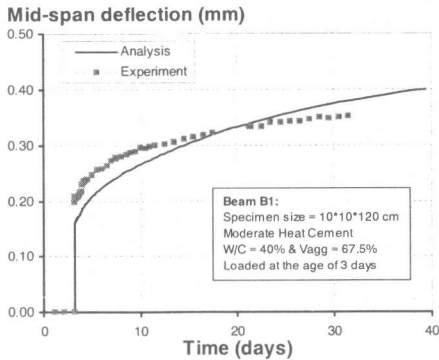


Fig. 8 Comparison between experimental and analytical results for case B1

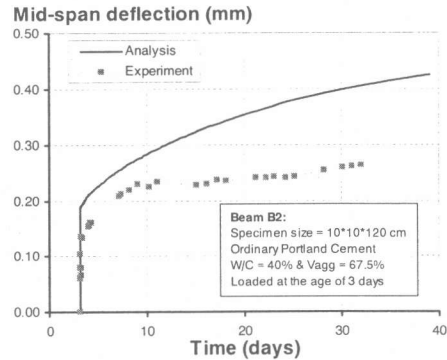


Fig. 9 Comparison between experimental and analytical results for case B2

The results for beam B1 and beam B2 are shown in Fig. (8) and Fig. (9), respectively. These two beams only differ in the type of cement used. It can be seen that good agreement occurs between the analytical results in case of B1 while the analytical results are overestimated in case of B2. The results for beams B3 and B4 are shown Fig. (10) and Fig. (11), respectively. Reasonable agreement is obtained in the case of B3 especially at the early age. In case of B4, the analytical results are rather

overestimated. From the above discussion, it can be seen that the proposed model can generally predict the deflection of concrete beams but, in some cases, further investigation is still required

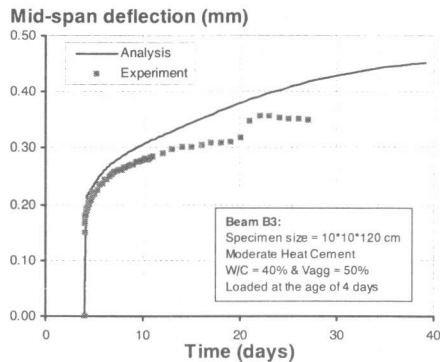


Fig. 10 Comparison between experimental and analytical results for case B3

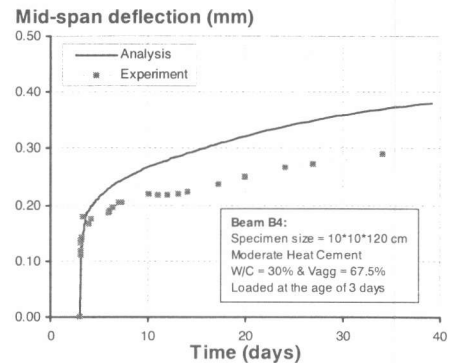


Fig. 11 Comparison between experimental and analytical results for case B4

4. CONCLUSIONS

A solidification model based on microphysical information for the prediction of both creep and shrinkage of hardening young concrete was presented. The solid model deals with cement paste as the solidified clusters having each creep property. Aggregates are idealized as suspended continuum media of perfect elasticity. The combination of both phases is used to represent the overall composite under unstable transient situations at early age. Further enhancements of the model parameters are done based on experimental work conducted on pure cement paste specimens. In order to verify the model properly, a series of experiments on concrete beams was conducted. The experimental results obtained are presented in this research and compared with the analytical results computed using the proposed model. The comparison between the analysis and the experiment shows acceptable agreement.

ACKNOWLEDGEMENTS

The first author is much grateful for TEPCO research foundation for their financial support.

REFERENCES

- [1] Mabrouk, R., Ishida, T. and Maekawa, K., "Solidification Model of Hardening Concrete Composite for Predicting Creep and Shrinkage of Concrete," JCI. Vol.20, 1998, pp. 691-696.
- [2] Mabrouk, R., "Unified Constitutive Law of Solidifying Concrete Composite for and Application to Reinforced Concrete Structures," Ph. D. thesis submitted to The University of Tokyo, 1999.
- [3] Bazant, Z. P., "Viscoelasticity of Solidifying Porous Material-Concrete" Journal of Engineering Mechanics ASCE. Vol. 103, 1977, pp. 1049-1067.
- [4] Maekawa, K., Chaube, R. P. and Kishi, T., "Coupled Mass Transport, Hydration and Structure Formation Theory for Durability Design of Concrete Structures," Proceedings of the International Workshop on Rational Design of Concrete Structures under Severe Conditions, 1995, pp. 263-274.
- [5] Maekawa, K., Chaube, R. and Kishi, T., "Modeling of Concrete Performance," E & FN SPON, 1999.
- [6] Shimomura, T. and Maekawa, K., "Analysis of the Drying Shrinkage Behavior of Concrete Using a Micromechanical Model Based on the Micropore Structure of Concrete," Concrete Library of JSCE No. 27, 1996, pp. 121-143.